

Excitation of bright and dark microwave magnetic envelope solitons in a resonant ring

Boris A. Kalinikos,^{a)} Nikolai G. Kovshikov,^{a)} and Carl E. Patton^{b)}
Department of Physics, Colorado State University, Fort Collins, Colorado 80523

(Received 25 February 1999; accepted for publication 17 May 1999)

The excitation of both bright and dark microwave magnetic envelope solitons has been realized for one and the same resonant ring containing a yttrium–iron–garnet film magnetostatic wave (MSW) delay line. The resonant ring modifies the MSW character to produce a series of frequency intervals with alternating regions of positive and negative dispersion. These alternating regions support bright and dark soliton production, respectively. © 1999 American Institute of Physics.
 [S0003-6951(99)02228-7]

The fundamental understanding of microwave magnetic envelope (MME) solitons has advanced significantly in recent years.^{1–7} The most recent advance was in the use of feedback techniques to produce long trains of such solitons from a single input pulse, or to self-generate bright and dark MME solitons even with no input pulse.^{5–7} MME soliton devices have potential for microwave signal processing applications. For example, they could be used to produce phase- and/or frequency-modulated signals for phase-shift keyed signal processing and related applications.

The feedback in Refs. 5–7 was obtained through a ring circuit composed of a yttrium–iron–garnet (YIG) film magnetostatic wave (MSW) delay line and an amplifier. The feedback was interrupted periodically to yield the reported soliton pulse trains. In each case, the YIG film was magnetized in the direction needed to produce the characteristic MSW dispersion for the desired type of soliton, bright or dark. The effect of the feedback on the dispersion was not considered; different structures were used to produce the bright or dark solitons.

This letter reports on the dual production of bright and dark solitons in one and the same YIG film resonant ring. This is possible because the ring, in addition to providing feedback, modifies the MSW dispersion such that frequency intervals with *both positive and negative dispersion* are obtained. Adjustment of the magnetic field, the input microwave pulse train repetition rate, and pulse width allows one to match the frequency spectrum of the input to the positive or negative dispersion regions and generate bright or dark solitons in the same circuit.

The experiments utilized a microwave pulse train input and a resonant ring structure as shown schematically in Fig. 1. For the bright pulse train with carrier frequency f_0 shown in (a), the repetition period T_R controls the frequency spacing of the peaks in the power spectrum of the input signal and the pulse width T_P controls the overall width of the power frequency spectrum.

For the resonant ring in (b), the orientation and value of the magnetic field H controls the MSW configuration and the

band of allowed MSW frequencies. The antenna spacing L controls the transit time for the individual MSW pulses in the YIG film delay line and the separation Δf between neighboring ring resonance frequencies. The field H in concert with the carrier frequency f_0 determines the frequency position of the input signal power spectrum of the input pulse train relative to the MSW ring resonances.

The delay line consists of a microstrip circuit with 50- μm -wide, 2-mm-long input and output transducers spaced 3 mm on a 50-mm-long, 2-mm-wide, and 5.2- μm -thick YIG film with unpinned surface spins. The amplifier and attenuator provided the feedback to obtain a high- Q multippeak ring resonance response. The microwave amplifier had a bandwidth greater than 2 GHz, a 30 dB dynamic range, and a high peak power. This ensured that the nonlinear ring response was determined solely by the YIG film response.

The orientation of the field H shown in Fig. 1(b) is in the plane of the YIG film and perpendicular to the MSW signal propagation direction. This corresponds to magnetostatic surface wave (MSSW) solitons. The results given below are for MSSW solitons at a carrier frequency f_0 of 5393.9 MHz. The repetition period T_R was set at 100 ns, for a power spectrum peak spacing of 10 MHz. For “bright” pulse experiments, T_P was set at 16 ns. For “dark” pulse experiments, the off-time, or $T_R - T_P$ was set at 22 ns. A field $H \approx 1180$ –1190 Oe provided the necessary match of the ring propagation time to the repetition period. As discussed be-

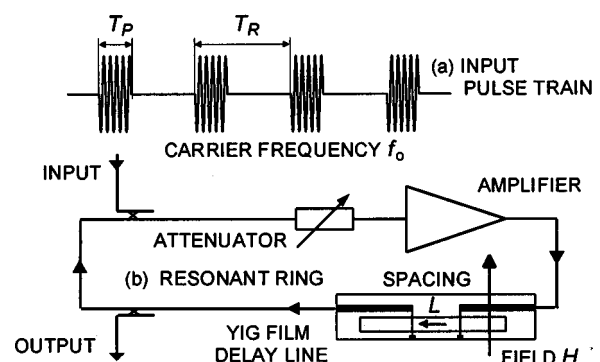


FIG. 1. Diagram of input microwave pulse train and magnetostatic wave resonant ring structure.

^{a)}Permanent address: St. Petersburg Electrotechnical University, 197376, St. Petersburg, Russia.

^{b)}Electronic mail: patton@lamar.colostate.edu

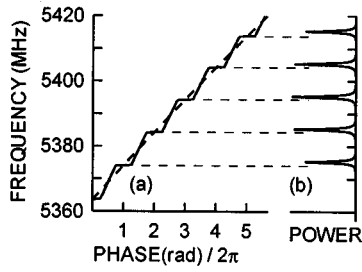


FIG. 2. Frequency vs phase dispersion curves and input signal power spectrum for a MSW ring resonator.

low, small adjustments in H were used to select out bright or dark solitons.

Similar results were also obtained for the magnetostatic backward volume wave (MSBVW) configuration with the field parallel to the propagation direction.

The concept behind the production of bright and dark solitons in one resonant ring is indicated in Fig. 2. Figure 2(a) shows schematic dispersion curves of carrier frequency f_c versus overall carrier phase shift ϕ_c around the ring. The dashed curve shows the dispersion due to the MSW response of the YIG film alone. The solid curve shows the actual computed dispersion when the feedback in the ring is taken into account. The curve shown is for typical experimental parameters as given above, a typical YIG film saturation induction of 1750 G, and an overall ring attenuation factor of 1 dB.

The details of the theory of this response will be published separately. In brief, one sets up an interference problem which combines the effect of the overall ring circulation and the frequency wave number operating point dependence of the MSW signal characteristics. The combined effect produces a modified functional dispersion character as shown in Fig. 2. This character resembles the original MSW dispersion but is modified significantly by the feedback.

The key modification of the original MSW dispersion is to produce crossing points. The crossing points of the solid and dashed curves at $\phi_c/2\pi = 1, 2, 3$ etc., correspond to the resonance frequencies of the ring. These resonance points are obtained from the phase-matching condition

$$\phi_c = k(f_c)L + \phi_e = 2\pi n, \quad (1)$$

where k is the YIG film MSW wave number at the frequency f_c , ϕ_e is the phase associated with the electronic part of the ring, and n is an integer.

Figure 2(b) shows a schematic power spectrum for a train of microwave pulses with a repetition period of 100 ns. The spectrum is shown relative to the common vertical frequency axis for the dispersion curves in Fig. 2(a). The spectrum is positioned so that the peaks fall slightly above the crossover points for the solid line feedback modified dispersion curves and the dashed line MSSW dispersion curves in (a).

The production of bright or dark soliton in one ring is based on the shape of the solid curve in Fig. 2(a). The frequency region just above each resonance point has positive curvature, while the region just below has negative curvature. Viewed as a dispersion curve of MSW frequency f_k

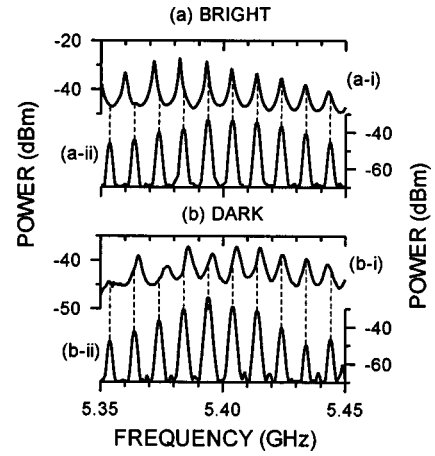


FIG. 3. Graphs (a) and (b) show power frequency characteristics for the bright and dark soliton configurations, respectively. Traces (a-i) and (b-i) show cw transmission loss vs frequency curves; (a-ii) and (b-ii) show power spectra for the bright and dark soliton pulse sequences, respectively.

versus wave number k , these regions correspond, therefore, to positive and negative values of the dispersion coefficient $D = (2\pi)^2 \partial^2 f_k / \partial k^2$, respectively.

The type of soliton which can be supported in a YIG film depends on the sign of the product of the dispersion coefficient D and the nonlinear response coefficient $N = 2\pi \partial f_k / \partial |u|^2$, where u represents the amplitude of the dynamic magnetization response. The N coefficient is negative for an in-plane magnetized film. Dispersion regions with $ND < 0$ support bright solitons and regions with $ND > 0$ support dark solitons. This means that frequencies just above the resonance points in Fig. 2 can support bright soliton trains; while frequencies just below the resonance points can support dark soliton trains.

The excitation of a sequence of a particular type of soliton is done as follows: First, one adjusts the input pulse repetition period T_R and the (f_0, H) operating point of the MSW line to match the frequency spacing of the peaks in the input pulse train power spectrum to the ring resonance frequency spacing Δf . Second, one makes a fine adjustment in the operating point frequency or the field to position the peaks in the input signal power spectrum just above or just below the ring resonance frequency points.

The actual measurements for a given configuration were carried out in two stages. First, the linear transmission-loss and phase versus frequency characteristics of the ring structure were measured at low cw power. These data yielded the dispersion properties of the ring, and, in particular, the ring resonance frequency points indicated in Fig. 2. Second, the input pulse power spectrum was matched to the dispersion and the desired sequence of solitons was generated. The data shown below were obtained for both soliton configurations, bright and dark, with ring gain factors of -1 and -4 dB, respectively. These gain factors were determined empirically, with a gain of 0 dB defined as the point at which the ring would just break into oscillation.^{6,7}

Figure 3 shows typical results for the MSSW measurements. Figure 3(a) is for bright solitons and an input pulse-dispersion match up as in Fig. 2. The field was 1183.2 Oe. Trace (a-i) gives the cw transmission-loss characteristic for the ring. The sharp cusps mark the ring resonance points. As

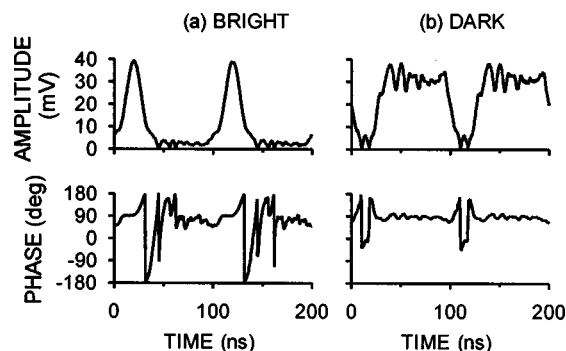


FIG. 4. Graphs (a) and (b) show amplitude and phase profiles for bright and dark solitons generated in the resonant ring, respectively.

described above, the input signal carrier frequency f_0 was set to position the peaks in the power spectrum of the input pulse train just above the cusp points in trace (a-i). Trace (a-ii) shows the power spectrum of the bright soliton train, which is generated in the ring.

Figure 3(b) shows parallel results for dark solitons. The field was 1186.3 Oe. The peaks in the cw transmission-loss profile in trace (b-i) are more rounded and do not have the sharp cusps evident from trace (a-i). This is due to the reduced gain factor, relative to the -1 dB value for trace (a-i). For dark solitons, the input pulse train was configured with the pulse off-time $T_R - T_P$ set at 22 ns, and f_0 was set to position the peaks in the power spectrum of the input pulse train just below the resonance peaks in trace (b-i).

The characteristics of the power spectra in traces (a-ii) and (b-ii) will be discussed shortly. First, however, it will prove useful to consider the actual temporal amplitude and phase profiles of these output signals. Figure 4 shows these profiles. The graphs under (a) and (b) show amplitude and phase versus time profiles for the bright pulse and the dark pulse experiments, respectively.

The graphs under (a) in Fig. 4 have the characteristics expected for bright solitons, a relatively narrow amplitude profile, and a phase profile which is constant across the pulse. The phase versus time profile has the critical constant phase signature for a bright soliton.⁵⁻⁷ Similarly, the graphs under (b) have the characteristics expected for dark solitons. The amplitude profile shows a characteristic dip with a pronounced double cusp and the phase profile shows two distinct 180° jumps associated with these cusps. These are pre-

cisely the established characteristics for pairs of dark solitons.⁸⁻¹⁰

With the temporal profiles in Fig. 4 now conclusively associated with bright and dark solitons, the power spectra for these signals in traces (a-ii) and (b-ii) of Fig. 3 are seen to have particular significance. For the bright soliton train, the peaks in the power spectra in trace (a-ii) fall just to the right of the cusps in the transmission-loss characteristic in trace (a-i). This positioning corresponds to regions of positive dispersion, as required for bright soliton production. For the dark soliton train, the peaks in the power spectra in trace (b-ii) fall just to the left of the peaks in the transmission-loss characteristic in trace (b-i). This positioning corresponds to regions of negative dispersion, as required for dark solitons.

In conclusion, this letter reports results on the continuous excitation of the bright and dark soliton trains in one and the same resonant ring. The specific data are for magneto-static wave solitons at microwave frequencies. The result, however, is very general. These same processes for bright and dark MSW soliton train excitation should be valid for a wide variety of resonant rings which support the propagation of dispersive nonlinear waves.

This work was supported in part by the U.S. Army Research Office, Grant No. DAAG55-98-1-0430; the National Science Foundation, Grant No. DMR-9801649; the Russian Foundation for Basic Research, Grant No. 96-02-19515; and the NATO Linkage Grant Program, Grant No. HTECH.LG970538.

¹ B. A. Kalinikos, N. G. Kovshikov, and A. N. Slavin, Zh. Eksp. Teor. Fiz. **94**, 159 (1988) [Sov. Phys. JETP **67**, 303 (1988)].

² M. Chen, M. A. Tsankov, J. M. Nash, and C. E. Patton, Phys. Rev. B **49**, 12773 (1994).

³ R. Marcelli and P. DeGasperis, IEEE Trans. Magn. **30**, 26 (1994).

⁴ N. G. Kovshikov, B. A. Kalinikos, C. E. Patton, E. S. Wright, and J. M. Nash, Phys. Rev. B **54**, 15210 (1996).

⁵ B. A. Kalinikos, N. G. Kovshikov, and C. E. Patton, Phys. Rev. Lett. **78**, 2827 (1997).

⁶ B. A. Kalinikos, N. G. Kovshikov, and C. E. Patton, Phys. Rev. Lett. **80**, 4301 (1998).

⁷ J. M. Nash, P. Kabos, R. Staudinger, and C. E. Patton, J. Appl. Phys. **83**, 2689 (1998).

⁸ A. N. Slavin, IEEE Trans. Magn. **31**, 3479 (1995).

⁹ S. A. Gredeskul and Yu. S. Kivshar, Opt. Lett. **14**, 1281 (1989).

¹⁰ B. A. Kalinikos, N. G. Kovshikov, and C. E. Patton, Pis'ma Zh. Eksp. Teor. Fiz. **68**, 229 (1998) [JETP Lett. **68**, 243 (1998)].